Metabolism-based scoring of cutaneous squamous cell carcinoma to predict tumour features and responses to treatment with dihydroorotate dehydrogenase inhibitors

Lea Dousset, Ferial Khalife, Domitille Chalopin-Fillot, Benjamin Dartigues, Fatima Naji, Walid Mahfouf, Elodie Muzotte, Benoît Rousseau, Nivea Amoedo, Stéphane Claverol, et al.

Br J Dermatol 2025; **193**:936–947
https://doi.org/10.1093/bjd/ljaf253
Advance access publication date: 27 June 2025

BJD
British Journal of Dermatology
Translational Research

Metabolism-based scoring of cutaneous squamous cell carcinoma to predict tumour features and responses to treatment with dihydroorotate dehydrogenase inhibitors

Lea Dousset,[1,2] Ferial Khalife,[1] Domitille Chalopin-Fillot,[3] Benjamin Dartigues,[3] Fatima Naji,[1] Walid Mahfouf,[1] Elodie Muzotte,[1] Benoît Rousseau,[4] Nivea Amoedo,[5,6] Stéphane Claverol,[7] Mathieu Bondaz,[8] Fanny Beltzung,[9] Marie-Laure Jullie,[9] Beatrice Vergier,[9] Alain Taieb,[1] Laure Favot-Laforge,[10] Rodrigue Rossignol,[5,6] Marie Beylot-Barry,[1,2] Macha Nikolski[3] and Hamid-Reza Rezvani[1,11]

[1]University of Bordeaux, Inserm, BRIC, UMR 1312, Bordeaux, France
[2]Dermatology Department, Bordeaux University Hospital, Saint-André Hospital, Bordeaux, France
[3]University of Bordeaux, CNRS, IBGC, UMR 5095, Bordeaux, France
[4]Animalerie A2, University of Bordeaux, Bordeaux, France
[5]Inserm U1211 Maladies Rares: Génétique et Métabolisme (MRGM), University of Bordeaux, Bordeaux, France
[6]CELLOMET, Bordeaux Centre of Functional Genomics, University of Bordeaux, Bordeaux, France
[7]University of Bordeaux, Bordeaux Proteome, Bordeaux, France
[8]Department of Oral and Maxillofacial Surgery, University of Bordeaux, Bordeaux, France
[9]Pathology Department, Bordeaux University Hospital, Haut-Lévêque Hospital, Pessac, France
[10]LITEC UR15560, Poitiers, France
[11]Aquiderm, University of Bordeaux, Bordeaux, France

Correspondence: Hamid-Reza Rezvani. Email: hamid-reza.rezvani@u-bordeaux.fr

Abstract

Background Alteration in metabolic activities is a critical step in cancer progression. Myriad metabolic-based therapy options are increasingly being proposed for human tumours. However, emerging evidence highlights interpatient metabolic heterogeneity and underscores the importance of metabolic phenotyping in cancer treatment.

Objectives To investigate metabolic heterogeneity in cutaneous squamous cell carcinoma (cSCC) and its impact on cSCC characteristics and treatment responses.

Methods We applied combined proteomic and bioenergetic analyses to patient samples representing various stages of cSCC, ranging from precancerous actinic keratosis to metastatic cSCC. To investigate the functional impacts of the identified metabolic heterogeneities on tumour characteristics and treatment responses, we used patient-derived tumour cell (PDC) and patient-derived xenograft (PDX) models by transplanting tumour cells and freshly resected patient tumours into immunocompromised mice.

Results Three subgroups with low, medium and high metabolic scores, respectively, were identified across all stages of carcinogenesis. Functional analyses indicated that, in both models (PDC and PDX), the sensitivities of tumours to leflunomide, an inhibitor of dihydroorotate dehydrogenase (DHODH), were inversely correlated with their metabolic scores and directly correlated with DHODH protein expression level. Moreover, DHODH overexpression in nonresponding groups rendered them sensitive to leflunomide.

Conclusions The findings demonstrate the relevance of metabolic profiling and scoring in the design of therapeutic approaches targeting the bioenergetic vulnerabilities of tumours and suggest DHODH as a promising therapeutic target in the low metabolic score subgroup of cSCC.

Accepted: 23 June 2025

Lay summary

Cutaneous squamous cell carcinoma (cSCC) is the second most common type of skin cancer. The number of cases is rising due to ageing populations and exposure to UV light. Most patients with cSCC have a good outcome. But, aggressive forms of cSCC can lead to poor outcomes and even death. We need new treatments and ways to find patients with cSCC who may respond well to specific therapy. Cancer cell metabolism is the way in which tumour cells generate energy. This plays a crucial role in how cancer cells behave and respond to treatment.

In this study, we created a metabolic scoring system to classify cSCC tumours. We investigated how these scores relate to tumour characteristics and treatment responses. Using cSCC samples and comparing them to healthy skin, we found three cSCC subgroups. These subgroups had low, medium and high metabolic scores. cSCC tumours with low metabolic scores responded better to a drug called 'leflunomide'. Leflunomide targets a key enzyme in metabolism called 'dihydroorotate dehydrogenase' (DHODH). cSCC tumours became sensitive to leflunomide when the levels of DHODH were higher.

A metabolic scoring system could help personalize treatment for patients with cSCC. It may help find people who respond well to treatments targeting tumour metabolism. Treatments that target DHODH are promising in cSCC tumours with low metabolic scores.

What is already known about this topic?

- Alteration in metabolic activities is a critical step in cancer progression.
- Metabolic reprogramming occurs at an early stage of ultraviolet B (UVB)-induced tumorigenic transformation of keratinocytes in chronically irradiated SKH-1 mice.
- Dihydroorotate dehydrogenase (DHODH) was found to be upregulated in UVB-induced cutaneous squamous cell carcinoma (cSCC).
- Treatment of mice with leflunomide (an inhibitor of DHODH) blocked UVB-induced cSCC formation.

What does this study add?

- Proteomic-based metabolic profiling defines three distinct bioenergetic subgroups of cSCC with low, medium and high metabolic scores, respectively, across all stages of carcinogenesis.
- Sensitivity of human cSCC to leflunomide is inversely correlated with metabolic scores.
- DHODH expression levels are inversely correlated with a tumour's metabolic score.
- Increasing DHODH expression in nonresponding groups sensitizes them to leflunomide.

What is the translational message?

- Metabolic profiling and scoring are key for designing therapeutic approaches targeting the bioenergetic vulnerabilities of tumours.
- Energy metabolism score and DHODH expression level serve as predictive markers for sensitivity to leflunomide treatment.
- DHODH is a promising therapeutic target in the low metabolic score subgroup of cSCC.

Cutaneous squamous cell carcinoma (cSCC) is the second most common nonmelanoma skin cancer, with a rising incidence due to population ageing and ultraviolet (UV) exposure.[1,2] It can manifest as a spectrum of progressively advanced malignancies, ranging from precursor actinic keratosis (AK) to *in situ*, invasive and, finally, metastatic cSCC.[3] While most cases have a good prognosis, aggressive forms – especially in immunocompromised patients or when left untreated –can be fatal.[4,5] Despite updated European guidelines for identifying high-risk cases,[6–9] a recent study found that, among 190 patients with advanced cSCC, 58% initially presented with low-stage tumours (Tis, T1 and T2).[10] This highlights the need for new profiling methods and precision medicine approaches.

Metabolic reprogramming plays a key role in cancer development,[11] making tumour bioenergetic vulnerabilities a promising target for personalized therapy.[12,13] Tumours have varied metabolic profiles, with some favouring glycolysis (the Warburg effect)[14,15] and others relying on oxidative phosphorylation (OXPHOS).[16] Our earlier work revealed that metabolic reprogramming begins early in cSCC formation through the activation of dihydroorotate dehydrogenase (DHODH).[17] DHODH is a rate-limiting enzyme in *de novo* pyrimidine synthesis, converting dihydroorotate to orotate. It also contributes to the electron transport chain by reducing ubiquinone to ubiquinol.[18] DHODH is upregulated in UVB-induced tumours, and its inhibition by the US Food and Drugs Administration-approved drug leflunomide (LFN) blocks UVB-induced tumours.[19–21] These findings highlight DHODH as a promising target for cSCC prevention and treatment.

Bioenergetic vulnerability-based cancer therapies are gaining interest,[22] but studies show significant interpatient metabolic heterogeneities, highlighting the need for metabolic phenotyping in cancer therapy.[23,24] For instance, lung cancers with high mitochondrial respiration respond to fatty acid α-oxidation inhibition.[24,25] Similarly, Gentric *et al*. found that high OXPHOS ovarian cancer subgroups were

more responsive to conventional chemotherapies than low OXPHOS subgroups.[26]

In this study, we profiled the metabolism of cSCC samples across stages of carcinogenesis and identified three subgroups with low, medium, and high metabolic scores, respectively, even at the precancerous stage. Based on this heterogeneity, we hypothesized that sensitivity to DHODH inhibitors varies by subgroup. Using PDX and PDC models, we showed that DHODH inhibitor efficacy correlates with metabolic score, highlighting its potential for predicting treatment response.

Materials and methods

The MITOSKIN project is a translational prospective study conducted in the Dermatology Department of Bordeaux University Hospital. For this study, every patient presented with a suspected lesion at different stages of carcinogenesis (AK, cSCC *in situ*, invasive cSCC, locally advanced cSCC, recurrent cSCC and cutaneous metastasis of cSCC). They were subjected to two biopsies of the tumour (one in formol for histopathological analysis to confirm the diagnosis of AK or cSCC, the other frozen in liquid nitrogen) and one of healthy tissue (also frozen in liquid nitrogen). The main clinical features of the cohorts are summarized in Table S1 (see Supporting Information). The analyses of tumour samples were performed according to the relevant national law, which protects people taking part in biomedical research. The MITOSKIN study is registered with ClinicalTrials.gov (NCT04389112). Additional materials and methods are provided in Appendix S1 (see Supporting Information).

Results

Proteomic profiling reveals that certain metabolic processes are significantly enriched in differentially expressed proteins throughout cSCC progression

Developing innovative cancer treatments requires a comprehensive understanding of molecular and cellular changes during tumour progression. To identify key proteins and processes involved in driving cSCC development, we performed large-scale quantitative label-free differential proteomic analysis on skin samples from 60 patients at various stages of carcinogenesis: AK ($n=16$), cSCC *in situ* ($n=15$), invasive cSCC ($n=14$) and recurrent/metastatic cSCC ($n=15$) (Figure 1a; Table S1). For each patient, paired healthy tissue at least 5 cm from the tumour was also collected. The distribution of age, patient sex and anatomical tumour location are shown in Figure 1(b–d). A total of 5509 proteins were identified, with at least two unique peptides and a 1% false discovery rate. Of these, 170, 168, 177 and 176 differentially expressed proteins were discerned when comparing AK, cSCC *in situ*, invasive cSCC and recurrent/metastatic cSCCs, respectively, with their matched healthy skin (Figure 1e, f). Protein fold changes were calculated by comparing tumour and healthy tissues across patients, as detailed in the methods.

To identify potential biomarkers and molecular alterations associated with cSCC progression, we then looked for the proteins that (i) displayed consistent trends of up- or downregulation during cSCC development and (ii) exhibited significant differences between AK and recurrent/metastatic cSCC. Our analysis identified 93 such proteins with 60 downregulated and 33 upregulated in the latter stage (Figure 2a, b). We then conducted enrichment analysis using the Kyoto Encyclopedia of Genes and Genomes (KEGG) pathway and WikiPathways annotation terms via 'gprofiler2', an R package for gene list functional enrichment analysis and namespace conversion toolset (version 0.2.3). To pinpoint the most representative annotation terms associated with these differentially expressed proteins, we applied ORSUM (version 1.7.0), a Python-based enrichment filtering tool.[27] The top representative terms and their ranking quartiles are presented (Figure 2c, d). Analysis of the enriched terms revealed that metabolic processes, such as 'fatty acid metabolism', 'metabolic pathways' and 'pyruvate metabolism', are associated with cSCC tumour progression (Figure 2c, d).

Proteomic-based metabolic profiling defines three distinct bioenergetic subgroups of cSCC

Certain metabolic pathways, such as lipid metabolism, were identified as being altered during cancer progression. In contrast, key energy metabolism pathways – specifically OXPHOS, glycolysis and the tricarboxylic acid (TCA) cycle – did not exhibit significant enrichment in our analysis. This finding may suggest underlying metabolic heterogeneity among patients at different stages of carcinogenesis. To further investigate this hypothesis, the expression levels of proteins involved in OXPHOS, glycolysis, the TCA cycle and fatty acid β-oxidation pathways were compared between each patient's tumour and corresponding healthy tissue (Figure 3a). Based on these expression levels and using principal component analyses (K-means clustering), patients with AK, cSCC *in situ*, invasive cSCC and metastatic cSCC were classified into three metabolic subgroups (Figure 3b). We then calculated metabolic scores ($\text{MetScore}_{\text{pathway}}$) for these four pathways using sentiment analysis approaches,[28,29] as detailed in the 'Materials and methods' section (Figure 3c). The overall metabolic score for each tumour ($\text{MetScore}_{\text{Tumour}}$) was finally determined by averaging the scores from these four pathways, resulting in the identification of three metabolic subgroups – 'low', 'medium' and 'high' metabolic profiles – within each clinicopathological stage (Figure 3c, d). A comparison of the $\text{MetScore}_{\text{Tumour}}$ across these three defined metabolic profiles found significant differences between the groups (Figure 3d).

We then analysed the metabolic canonical pathways to identify those that could serve as prognostic metabolic markers. To this end, mean metabolic scores for each pathway were calculated within each of the three metabolic profiles ('low', 'medium' and 'high'), resulting in three mean values per pathway. To select pathways that distinguish between the three metabolic profiles, we used the monotonic function in the R package 'MonoInc' (1.1), which assesses whether a series of values is monotonic and increasing. Pathways that exhibited increasing monotonicity from 'low' to 'medium' to 'high' were selected (Figure S1, Table S2; see Supporting Information). Applying the $\text{MetScore}_{\text{Tumour}}$ calculation to these prognostic metabolic pathways revealed that patients

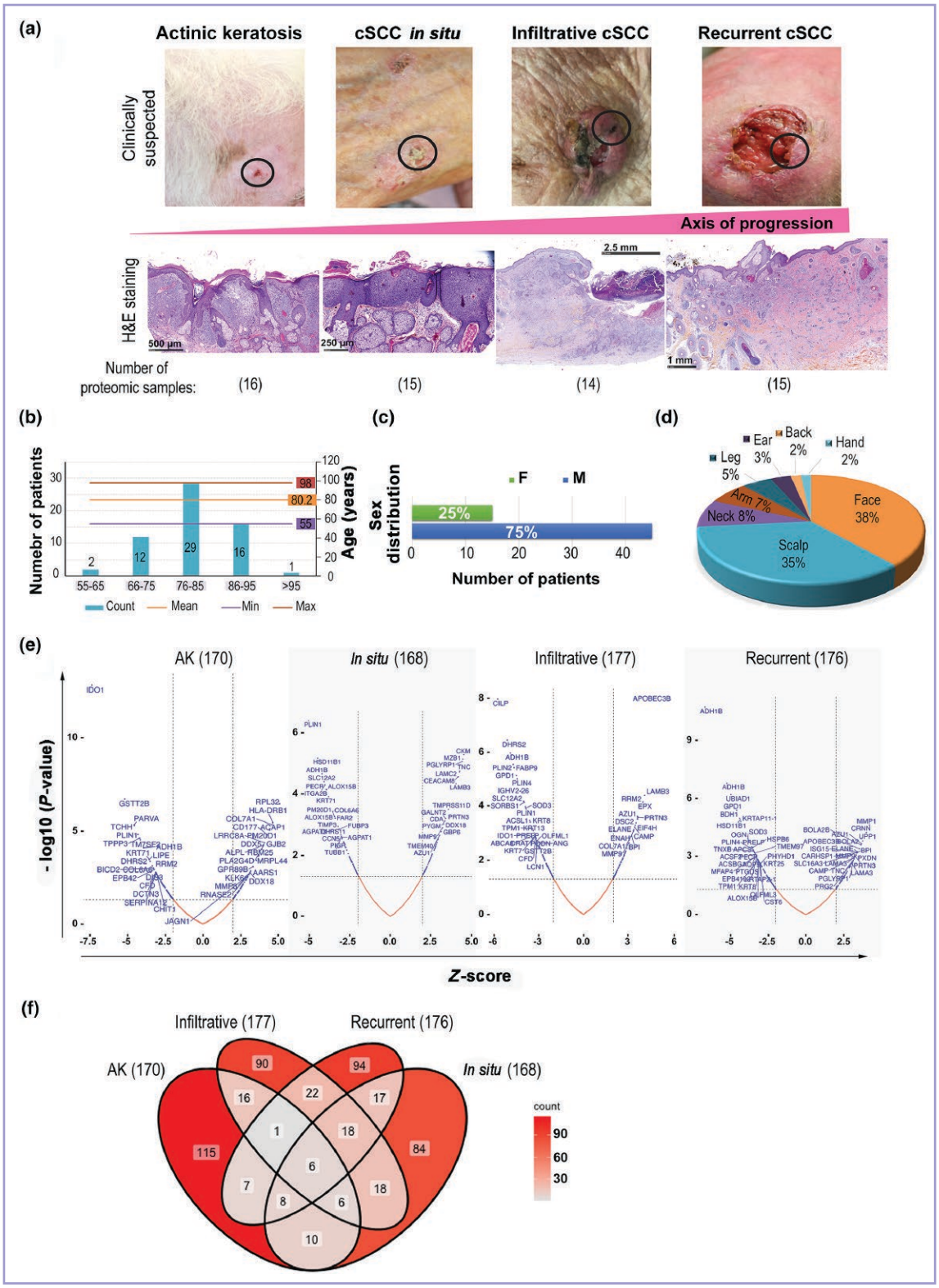

Figure 1 Fewer than 200 proteins were differentially expressed at different stages of cutaneous squamous cell carcinoma (cSCC) progression. (a) Schematic representation of cSCC progression ranging from (left to right) actinic keratosis (AK) to cSCC *in situ* to invasive cSCC and to metastatic/recurrent cSCC. A comprehensive label-free proteomic study was performed on 16 AKs, 15 cSCC *in situ*, 14 infiltrative cSCCs, 15 recurrent/metastatic cSCCs and their respective healthy tissues (n=120). (b, c, d) The distribution of age, patient sex and anatomical tumour location are shown. (e) Volcano plots show the differentially expressed proteins (DEPs) vs. their corresponding healthy skin samples. A total of 170, 168, 177 and 176 DEPs were identified in AKs, cSCC *in situ*, invasive cSCCs and recurrent/metastatic cSCCs, respectively. (f) A Venn diagram was applied to present the common DEPs among the groups. Among these, seven common DEPs were detected across all stages of cSCC. F, female; H&E, haematoxylin and eosin; M, male.

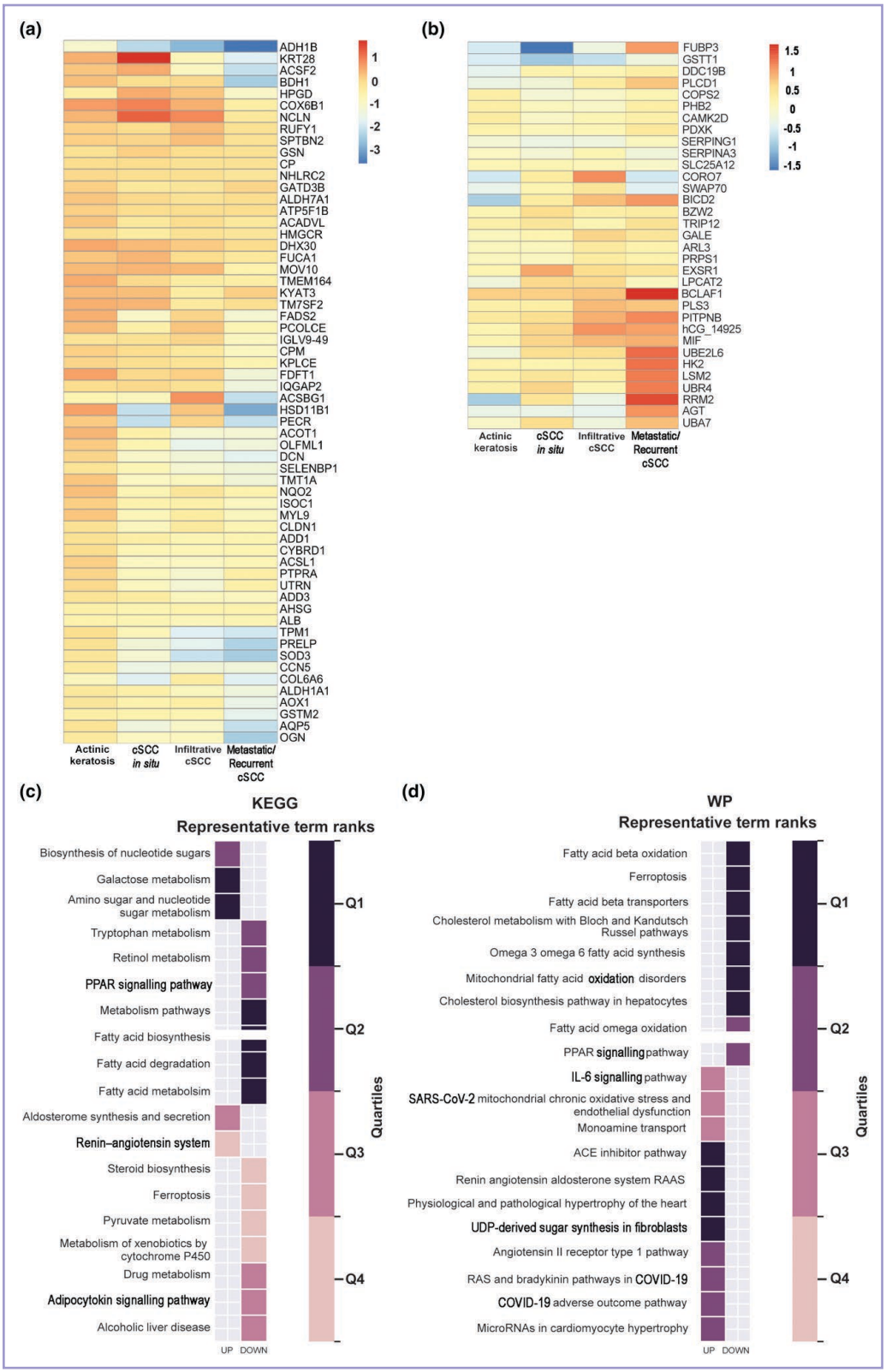

Figure 2 Proteome enrichment analysis reveals that metabolic processes are associated with differentially expressed proteins throughout cutaneous squamous cell carcinoma (cSCC) progression. (a) The heatmap on the left represents 60 proteins whose expression levels tend to decrease throughout cSCC development, while (b) the heatmap on the right shows 33 proteins with a tendency to increase throughout cSCC development. (c) Kyoto Encyclopedia of Genes and Genomes (KEGG) and (d) WikiPathways (WP) enrichment analyses were performed on the 93 differentially expressed proteins. After applying ORSUM filtering, the top representative terms and the rank quartiles are presented. ACE, angiotensin converting enzyme; IL-6, interleukin 6; PPAR, peroxisome proliferator-activated receptor; UDP, uridine diphosphate.

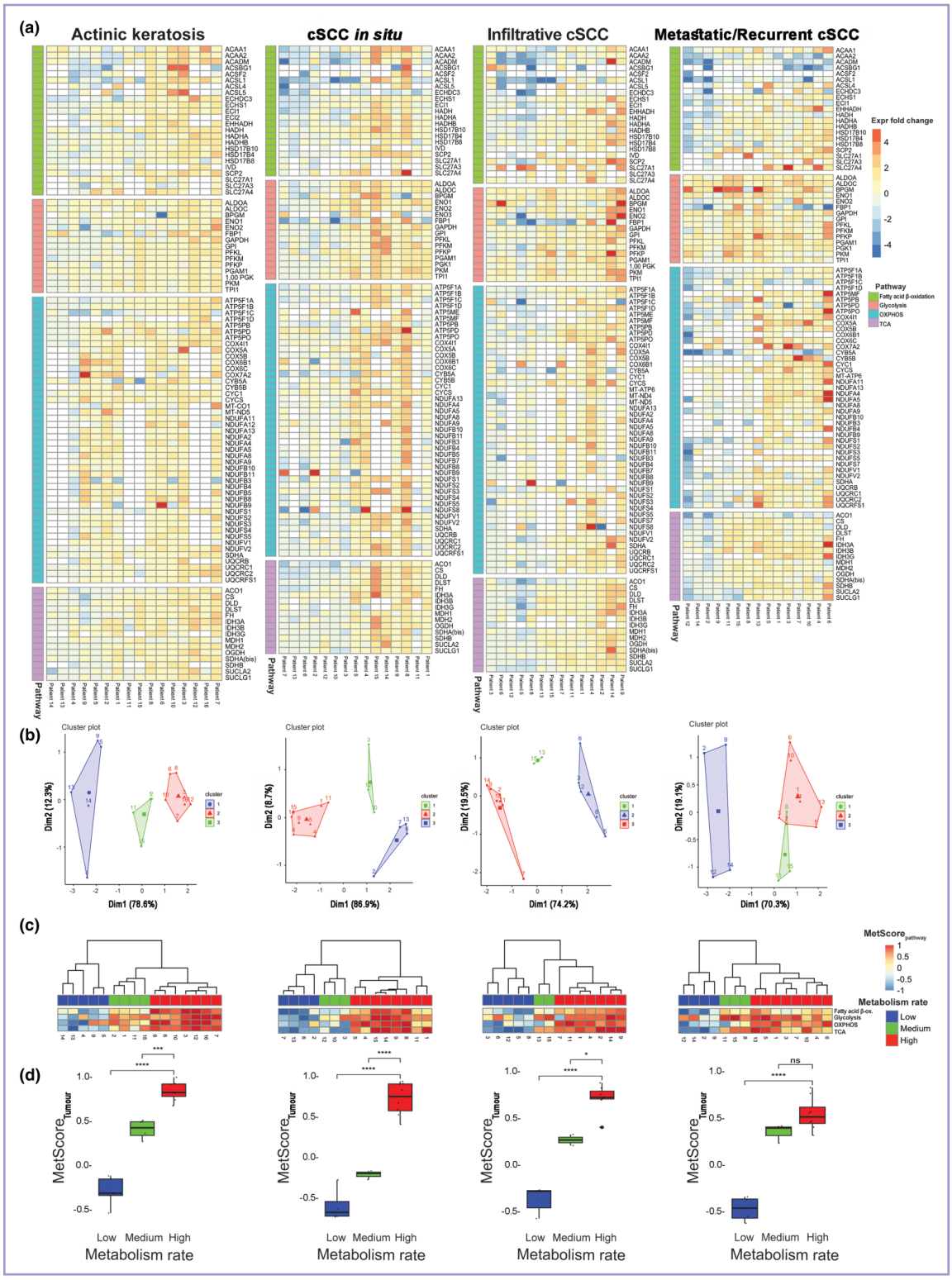

Figure 3 Metabolic heterogeneity among human cutaneous squamous cell carcinomas (cSCCs) at different stages of carcinogenesis. (a) Heatmap shows the fold change in the expression levels of proteins involved in oxidative phosphorylation (OXPHOS), glycolysis, the tricarboxylic acid (TCA) cycle and fatty acid β-oxidation in human patient lesions vs. their respective healthy skin. Each column represents a sample and each row represents a protein. Downregulated proteins are shown in blue, upregulated proteins in red and unchanged proteins in white. (b) K-means clustering was performed to classify the patients into three groups. (c) Metabolic scores for each pathway ($MetScore_{pathway}$) were calculated for OXPHOS, glycolysis, the TCA cycle and fatty acid β-oxidation, as detailed in the 'Materials and methods'. Patients with low, medium and high metabolic rate cSCC [based on the consensus k-means clustering in (b)] are coloured blue, green and red, respectively. (d) The metabolic score for each tumour ($MetScore_{Tumour}$) was determined by averaging the metabolic scores of the four mentioned pathways and presented in a boxplot. $MetScore_{Tumour}$ were compared among low, medium and high metabolic score groups. *P*-values were obtained from a one-way ANOVA test. ns, not significant (i.e. $P > 0.05$). *$P < 0.05$; ***$P < 0.001$; ****$P < 0.0001$.

in the high metabolic rate subgroup had significantly higher scores than those in the low metabolic rate subgroup at all stages of carcinogenesis (Figure S1a, b). Notably, most of these pathways are involved in energy production, lipid metabolism, amino acid metabolism or NAD^+ bioavailability. The consistent up- or downregulation of these pathways across the identified metabolic subgroups suggests a coordinated metabolic adaptation.

To assess whether the MetScores reflect the functional metabolic characteristics of tumours, biochemical functional analyses were conducted on selected infiltrative cSCC tumours and their corresponding healthy tissues. Tumours with low MetScores exhibited reduced glucose uptake, oxygen consumption rate and mitochondrial complex IV activity vs. their matched healthy tissues. In contrast, those with high MetScores demonstrated increased levels of these metabolic functions relative to their corresponding healthy tissues (Figure S2; see Supporting Information). Overall, our results revealed significant metabolic heterogeneity among cSCC samples and identified three distinct bioenergetic subgroups at every stage of cSCC carcinogenesis.

Sensitivities of human cSCC patient-derived xenografts to leflunomide were dependent on the energy metabolism score of primary human tumours

To examine the functional impact of the identified metabolic heterogeneities on tumour treatment responses, we investigated the effect of LFN on patient-derived xenografts (PDXs) of human cSCCs with different metabolic scores. Of note, LFN was selected based on our previous findings, which showed that DHODH represents a metabolic vulnerability that could be targeted to inhibit cSCC progression due to its pivotal role in the interplay between several metabolic pathways (e.g. OXPHOS, nucleotide biosynthesis, ATP synthesis and redox signalling) (Figure 4a).[17,21] To establish a PDX biobank of human cSCC, tissue samples were processed within 1 h of biopsy and implanted subcutaneously into NSG® mice. A portion of these samples was also subjected to proteomic analysis. Thirty samples were successfully engrafted, including 2 normal-appearing skin samples from UV-exposed areas, 5 AKs, 7 cSCC *in situ*, 12 invasive cSCCs and 3 locally advanced cSCCs (F1). While none of the healthy-appearing skin samples or AK samples demonstrated growth in the F1 engraftment, successful growth was observed in 1 of 7 (14%) cSCC *in situ*, 4 of 12 (33%) invasive cSCCs and 2 of 3 (66%) locally advanced cSCCs. These successfully engrafted samples were then reimplanted into NSG mice (F2) and maintained through serial passaging for more than three generations (≥ F3) (Figure 4b).

To investigate whether the effect of LFN depends on the energy metabolism score, three successfully engrafted invasive cSCC samples, initially scored as low, medium and high metabolism ($MetScore_{Tumour}$ values of −0.45, 0.33 and 0.88, respectively), were transplanted into eight mice (Figure 4b). When tumours reached 200 mm^3, vehicle and LFN were administered orally. Interestingly, tumours derived from a low MetScore cSCC were susceptible to LFN, whereas those derived from a medium MetScore cSCC were less sensitive and tumours derived from a high MetScore cSCC showed no sensitivity to LFN (Figure 4c).

To assess the link between LFN sensitivity and DHODH expression, Western blot analysis was performed. Tumours with low and medium MetScores had higher DHODH protein levels than their corresponding healthy tissues, whereas high MetScore tumours exhibited reduced DHODH expression (Figure 4d). Further analysis of eight additional cSCC samples revealed consistently higher DHODH levels in low MetScore tumours vs. matched healthy tissues, while high MetScore tumours displayed reduced or unchanged expression (Figure 4e, f). Taken together, our results demonstrate that the sensitivity of PDXs to LFN treatment depends on their metabolic score and level of DHODH expression.

Metabolic profiles of cells dictate the inhibitory efficacy of leflunomide on tumour growth and their metastatic potential

We used six cSCC cell lines isolated from different stages of carcinogenesis (Figure S3a, Table S3; see Supporting Information). MET1, MET2 and MET4, representing distinct stages of carcinogenesis, were isolated from a patient who had a kidney transplant. IC1MET cells were isolated from a patient with metastatic cSCC, while IC12 and IC18 cells were from invasive cSCC (Figure S3a).

To characterize the metabolic features of these cell lines, a label-free proteomic approach was applied, similar to that used for human tumours. Using the same analytical method, we classified them into three categories with low, medium and high MetScores (Figure S3b). To evaluate their metastatic potential, these cell lines were transduced with a lentiviral vector expressing luciferase before xenografting. After transplantation into mice and once the tumours reached an average volume of 200 mm^3, mice were divided into two groups: one group received vehicle alone and the other LFN. After monitoring tumour growth for 1 month, the tumours were resected and the mice underwent imaging 1 week later to detect metastasis (Figure S3c). Treatment with LFN was well tolerated by the mice: no loss of bodyweight was seen (Figure S3d), and there was no difference in behaviour among the different groups. The results showed that LFN treatment significantly reduced the growth of IC1MET and MET2 tumours (Figure S3e), as well as the specific growth rate (SGR; Figure S3f). In contrast, MET4 and IC12 tumours continued to grow, with no significant difference in tumour growth rates between the vehicle- and LFN-treated groups (Figure S3e, f).

Histological examination of resected tumours revealed that vehicle-treated IC1MET and MET2 tumours were less differentiated than LFN-treated tumours (Figure S4A; see Supporting Information). This difference in differentiation was not found between vehicle- and LFN-treated MET4 and IC12 tumours (Figure S4a).

Focusing on the effect of LFN treatment on the metastatic behaviour of these cells indicated that while all mice in the vehicle-treated IC1MET group developed metastases, only about 60% of mice in the LFN-treated IC1MET group did [Figure S4b, Table S4 (see Supporting Information)]. On the contrary, the percentage of mice with metastases was similar between vehicle- and LFN-treated MET4 groups (Figure S4b, Table S4). Notably, metastases were predominantly found in the inguinal and axillary lymph nodes, lungs and liver (Figure S4b, Table S4). No metastases were observed

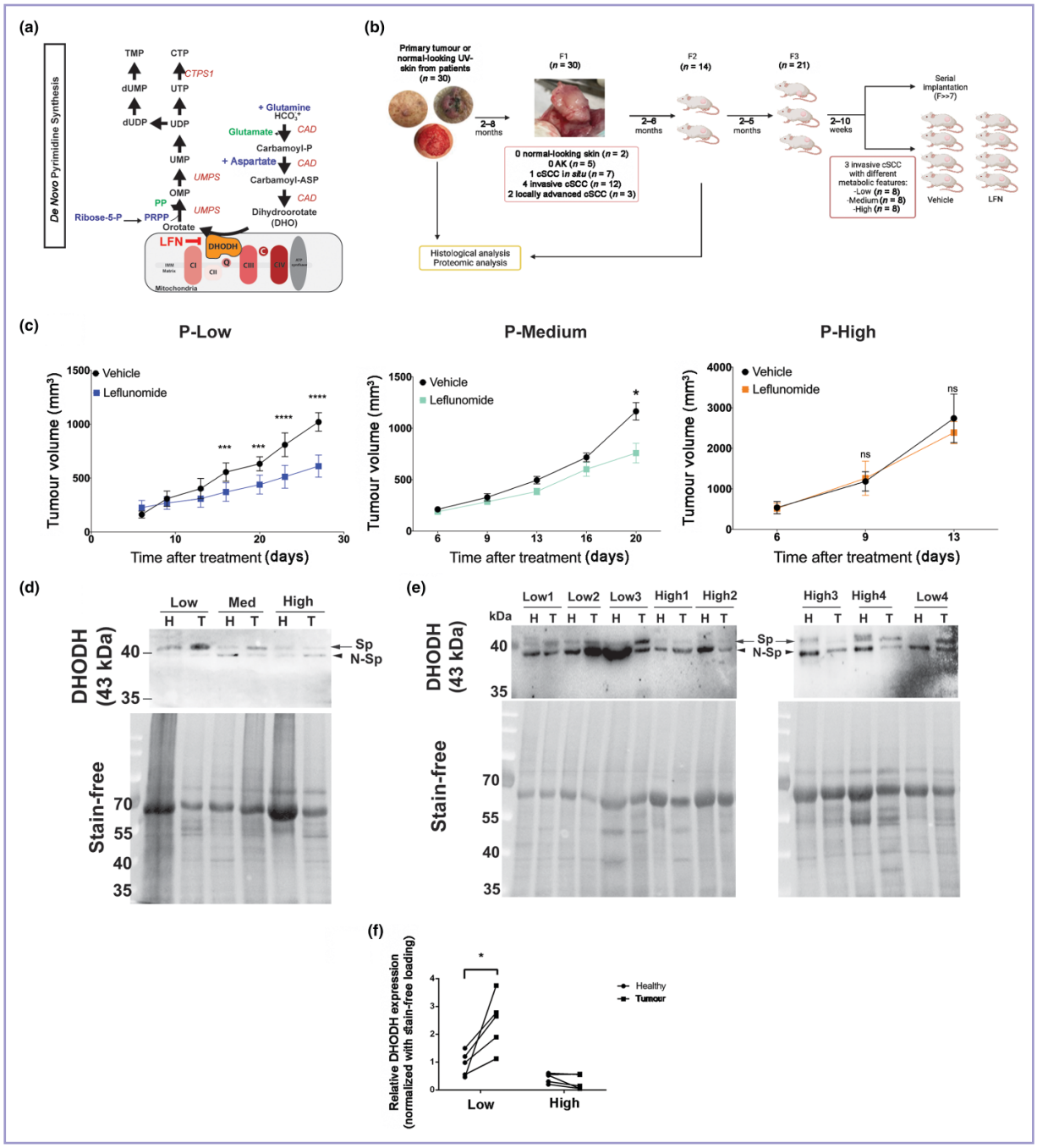

Figure 4 Treatment of patient-derived xenografts (PDXs) reveals that low metabolic score tumours are sensitive to dihydroorotate dehydrogenase (DHODH) inhibition. (a) Schematic illustrating the role of DHODH in *de novo* pyrimidine synthesis and oxidative phosphorylation (OXPHOS). (b) PDX models were established by transplanting freshly resected patient tumours into NSG® immunodeficient mice. Primary tumours collected from patients at different stages of carcinogenesis were used, including normal-looking ultraviolet-exposed-skin (n=2); actinic keratosis (AK; n=5); cutaneous squamous cell carcinoma (cSCC) *in situ* (n=7); invasive cSCC (n=12) and locally advanced cSCC (n=3). Only 7 of 30 PDXs were passageable for>3 passages (>>F3). (c) Punch biopsies taken from the F3 generation of three PDXs of invasive cSCC with low, medium and high metabolic scores were transplanted subcutaneously into 24 NSG mice (eight mice per group). When tumours reached 200 mm^3, mice were orally administered leflunomide (LFN) or carboxymethylcellulose [vehicle (veh)]. Tumour growth was monitored and measured in low, medium and high metabolic score tumours in vehicle- and LFN-treated mice (n=8 mice per group). *P<0.05, ***P<0.01, ****P<0.001. (d) Representative Western blot showing DHODH expression levels in cSCCs with low, medium and high metabolic scores, used in the PDX experiment, along with their corresponding healthy tissues. A stain-free gel was used as a loading control. (e) Western blot showing DHODH expression levels in four low and four high metabolic score cSCCs and their corresponding healthy tissues. A stain-free gel was used as a loading control. (f) DHODH protein levels in tumours and their corresponding healthy tissues [shown in panels (d) and (e)] were quantified. A stain-free gel was used to normalize sample loading. A two-way repeated measures ANOVA followed by Sidak's test showed that DHODH protein expression was significantly higher in tumours compared with matched healthy tissue in the low MetScore group (P<0.05) but not in the high MetScore group. CAD, carbamoyl-phosphate synthetase 2, aspartate transcarbamylase and dihydroorotase; CTP, cytidine triphosphate; dUDP, deoxyuridine diphosphate; dUMP, deoxyuridine monophosphate; H, healthy tissue; N-Sp, nonspecific band; OMP, orotidine 5′-monophosphate; PP, pyrophosphate; PRPP, phosphoribosyl pyrophosphate; Sp, specific band; T, cSCC tumour; TMP, thymidine monophosphate; UDP, uridine diphosphate; UMP, uridine monophosphate; UMPS, uridine monophosphate synthase; UTP, uridine triphosphate.

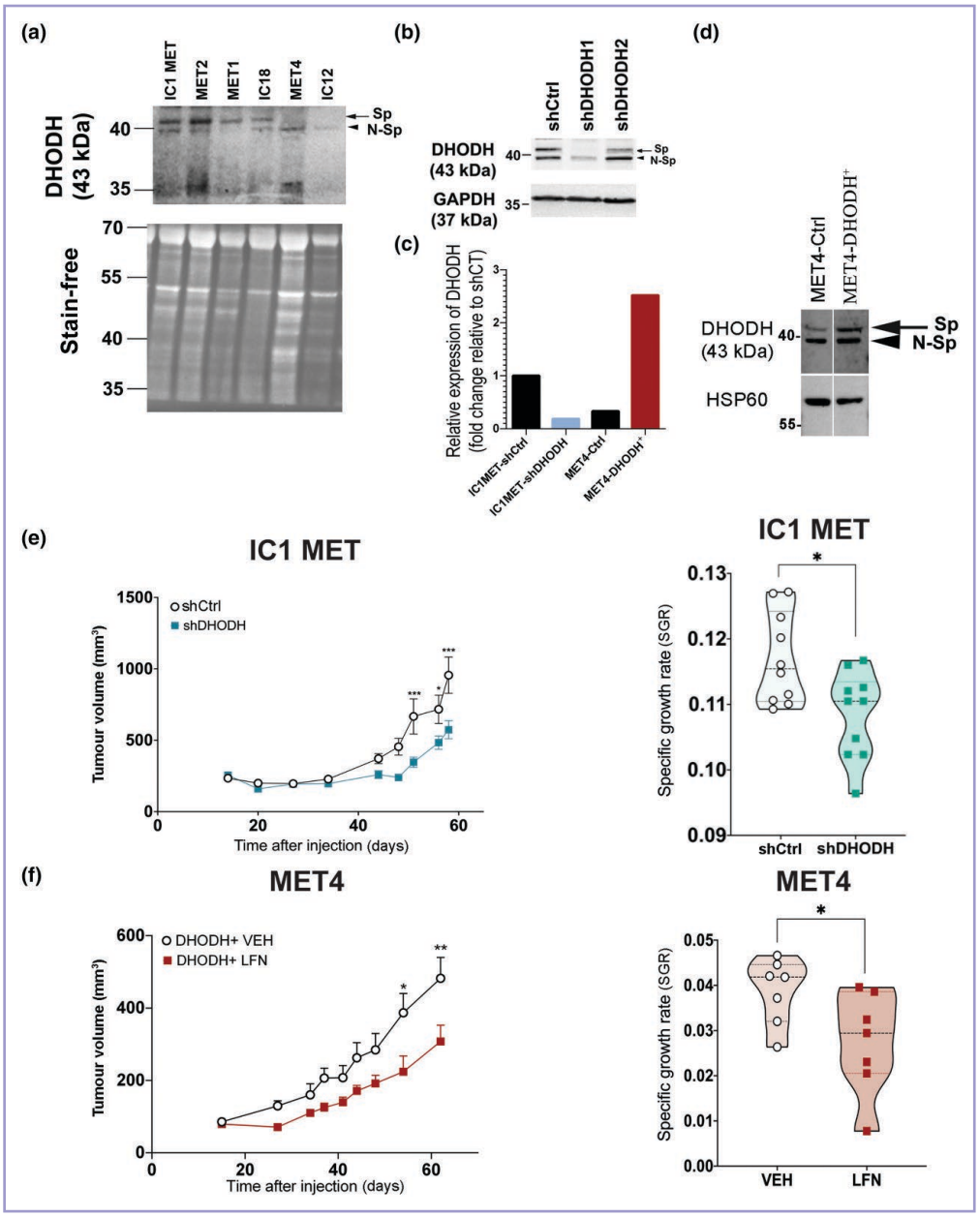

Figure 5 Overexpression of dihydroorotate dehydrogenase (DHODH) in nonresponder MET4 cells renders them sensitive to leflunomide (LFN) treatment. (a) A representative Western blot showing DHODH protein levels in MET1, MET2, MET4, IC1MET, IC12 and IC18 cells. A stain-free gel was used as a loading control. (b) The efficiency of different short hairpin (sh)DHODHs in reducing DHODH expression in IC1MET cells was tested by Western blot. GAPDH was used as a loading control. (c) DHODH mRNA expression levels were measured by quantitative reverse transcription polymerase chain reaction in IC1MET and MET4 cell lines. (d) DHODH was overexpressed following the transduction of MET4 cells with a lentiviral vector expressing DHODH. Heat shock protein 60 (HSP60) was used as a loading control. (e) IC1MET cell lines were transduced with lentiviral vectors expressing shControl (shCtrl) or shDHODH. Cells were transplanted into NSG® mice. Tumour growth rates (left) and specific growth rates (SGR; right) of shControl- and shDHODH-transduced IC1MET cells were assessed. Data are presented as mean (SEM). *P*-values were calculated using mixed-effect analysis ($n=10$). (f) MET4 cells were transduced with lentiviral vectors expressing DHODH. Cells were transplanted into NSG mice and then either treated with vehicle or LFN. Tumour growth rates (left) and SGR (right) of MET4 overexpressing DHODH (DHODH$^+$) treated with vehicle or LFN were assessed. Overexpression of DHODH sensitized these cells to LFN. Data are presented as mean (SEM). *P*-values were calculated using a two-way ANOVA ($n=7$). N-Sp, nonspecific band; Sp, specific band; VEH, vehicle. $^*P<0.05$; $^{**}P<0.01$; $^{***}P<0.001$.

in either treated or untreated xenografted mice with MET2 or IC12 cells (Table S4).

Finally, DHODH activity measurements across different groups showed significantly higher DHODH activity in xenografts from low metabolic score cells, which was markedly reduced by LFN treatment (Figure S4c). Taken together, our data suggest that LFN effectively limits tumour growth in the low metabolic score group.

Energy metabolism score and DHODH expression level serve as predictive markers for sensitivity to leflunomide treatment

To evaluate whether the sensitivity of these cell lines to LFN could also be attributed to the expression levels of DHODH, Western blotting was carried out (Figure 5a). DHODH protein expression levels in the cells with low and medium

metabolic scores were similar and were much higher than the levels found in MET4 and IC12 cells (Figure 5a). To further investigate, the expression of DHODH was downregulated in IC1MET cells and upregulated in MET4 cells using lentiviral vectors. Among different short hairpin (sh)DHODH constructs tested *in vitro*, shDHODH1 significantly reduced the DHODH expression, as shown in Figure 5(b, c). Lentiviral vector-mediated overexpression of DHODH in MET4 cells resulted in 2.53- and 3.43-fold increases at the mRNA and protein levels, respectively (Figure 5c, d). Six days after transduction, the cells were subcutaneously engrafted into NSG mice. A significant reduction in the kinetics of tumour growth rate and SGR were seen in the group that received shDHODH-transduced IC1MET cells compared with the group transplanted with shControl-transduced cells (Figure 5e). The average tumour volume in MET4 cells overexpressing DHODH, when treated with LFN, was significantly lower compared with those treated with the vehicle (Figure 5e), suggesting that DHODH upregulation sensitizes MET4 cells to LFN. Taken together, our results demonstrate that the sensitivity of cSCC cells to LFN treatment is determined by their metabolic score and DHODH expression level.

Discussion

Here, we present the largest proteomic analyses conducted on human cSCC to date, revealing an unexpected metabolic heterogeneity in samples at the same stage of cSCC progression. We have provided evidence that human cSCCs at different stages of carcinogenesis could be stratified based on their metabolic profiles, which significantly influence their responses to metabolism-based treatment. Our findings suggest that deciphering the functional status of energy metabolism pathways on punch biopsies using proteomic analyses could be a valuable approach to the metabolic profiling of cSCC in the clinical setting.

Genomic analyses have previously identified several mutational signatures and heterogeneity in significantly mutated genes in cSCC.[30–32] Interestingly, mutation signature patterns were similar in MET1, MET2 and MET4 cells, isolated from the same patient, with the exception that MET4 harboured an additional signature that was absent in the others.[32,33] However, our results demonstrate that these cells exhibit distinct metabolic features, in that MET2 was classified as a low metabolic score subgroup, MET1 as a medium metabolic score subgroup and MET4 as a high metabolic score subgroup (see Figure S3). Altogether, these data suggest that mutational analysis alone is insufficient and should be complemented by metabolic profiling to optimize the therapeutic strategy.[34]

DHODH inhibition has been shown to reduce the growth of various solid tumours, including highly aggressive small cell lung cancer, acute myeloid leukaemia, triple-negative breast cancers and UVB-induced cSCC.[17,35–47] Here, we showed that some cSCC cells are sensitive to DHODH inhibition in a metabolic score-dependent manner. An interesting question raised by these results is why tumours with low metabolic scores are sensitive to LFN, whereas those with high scores are not. As DHODH expression and activity levels are already low in cells with high MetScores, LFN treatment does not significantly reduce its activity, as shown in Figure S4(c). We could also hypothesize that in the high MetScore group, the simultaneous upregulation of all four major energy metabolism pathways may provide tumour cells greater metabolic flexibility, enabling them to compensate when one pathway is inhibited. Increased DHODH expression has been associated with shortened overall survival in patients with oral SCC, and DHODH inhibition has been shown to impair tumour growth in a xenograft model.[48] Mohamad-Fairus *et al*. have similarly demonstrated that DHODH expression levels play a critical role in determining the sensitivity of tumours to DHODH inhibitors.[49] Along this line, we showed that MET4 cells, in which the expression level of DHODH was low (Figure 5a), did not respond to LFN treatment, except when DHODH is experimentally overexpressed (Figure 5f). An important unanswered question of this work is whether DHODH upregulation can alter the MetScore of tumours.

Upregulation of the pyrimidine biosynthesis pathway has been observed in cells treated with genotoxic agents, such as chemotherapy components.[44,50] As this increase relies on the enhanced activity of DHODH – the pathway's rate-limiting enzyme – targeting DHODH may boost the effectiveness of treatments like programmed cell death 1 inhibitors or chemotherapy. In accordance with this hypothesis, we previously proposed combining 5-fluorouracil with LFN for cSCC.[21] Similar combinations, such as LFN with a MEK inhibitor for melanoma,[38] or with doxorubicin for breast cancer,[44] have also been proposed. Additionally, *in vivo* selection of patient-derived tumour xenografts with greater metastatic potential led to enrichment of tumour cells with upregulated pyrimidine biosynthesis, making them highly sensitive to LFN.[51]

Overall, our data indicate that the metabolic profiling of cSCCs could serve as a practical approach to managing advanced cSCCs with targeted therapeutic agents. We envision a future where patients with cSCC are stratified based on their metabolic profiles and DHODH expression levels, in particular in cases of clinically/histologically aggressive subtypes, as a crucial step in a precision medicine approach.

Acknowledgements

The authors wish to thank Dr Véronique Guyonnet-Duperat (TBMCore, Plateforme de Vectorologie, University of Bordeaux), Christine Alfaro (CHU Bordeaux, human sample collection), Dr Olivier Cogrel, Dr Jean-Michel Amici, Dr Paul Cirotteau (Dermatopathology, CHU Bordeaux), Professor Pierre Dubus and Professor Jean-Philippe Merlio (CRB Cancer).

Funding sources

H.R.-R. gratefully acknowledges support from the Institut National du Cancer 'INCa_2021-105', the 'Société Française de Dermatologie (SFD)', Fonds de Dotation pour la recherche de la SFD, the 'Fondation SILAB-Jean Peaufique', the 'Groupe de Cancérologie Cutané (GCC)' and the Fondation ARC pour la Recherche sur le Cancer (ARC, ARCPJA2022060005247). L.D. was supported by grants from the Institut National de la Santé et de la Recherche Médicale (INSERM) and the University Hospital of Bordeaux.

Conflicts of interest

The authors declare no conflicts of interest.

Data availability

The authors declare that the data supporting the findings of this study are available within the paper and its Supporting Information. The proteomics data have been deposited to the ProteomeXchange Consortium via the PRIDE partner repository with the dataset identifier PXD044995. Additional data are available from the corresponding author upon reasonable request.

Ethics statement

The National Commission for Data Processing and Liberties approved all analyses realized in this study (approval no.: ID-RCB 2018-A03096, delivered on 4 January 2019). The MITOSKIN study was registered with ClinicalTrials.gov (NCT04389112). All mouse experiments were conducted in accordance with the approval of the Bordeaux University Animal Care and Use Committee.

Patient consent

Patients/participants provided written informed consent to take part in the study. In cases of patient refusal, expressed either orally or in writing, residual tumour samples were excluded.

Supporting Information

Additional Supporting Information may be found in the online version of this article at the publisher's website.

References

1 Rogers HW, Weinstock MA, Feldman SR, Coldiron BM. Incidence estimate of nonmelanoma skin cancer (keratinocyte carcinomas) in the US population, 2012. *JAMA Dermatol* 2015; **151**:1081–6.
2 Donaldson MR, Coldiron BM. No end in sight: the skin cancer epidemic continues. *Semin Cutan Med Surg* 2011; **30**:3–5.
3 Ratushny V, Gober MD, Hick R *et al.* From keratinocyte to cancer: the pathogenesis and modeling of cutaneous squamous cell carcinoma. *J Clin Invest* 2012; **122**:464–72.
4 Brantsch KD, Meisner C, Schönfisch B *et al.* Analysis of risk factors determining prognosis of cutaneous squamous-cell carcinoma: a prospective study. *Lancet Oncol* 2008; **9**:713–20.
5 García-Foncillas J, Tejera-Vaquerizo A, Sanmartín O *et al.* Update on management recommendations for advanced cutaneous squamous cell carcinoma. *Cancers* 2022; **14**:1–19.
6 Kandolf L, Peris K, Malvehy J *et al.* European consensus-based interdisciplinary guideline for diagnosis, treatment and prevention of actinic keratoses, epithelial UV-induced dysplasia and field cancerization on behalf of European Association of Dermato-Oncology, European Dermatology Forum, European Academy of Dermatology and Venereology and Union of Medical Specialists (Union Européenne des Médecins Spécialistes). *J Eur Acad Dermatol Venereol* 2024; **38**:1024–47.
7 Stratigos AJ, Garbe C, Dessinioti C *et al.* European consensus-based interdisciplinary guideline for invasive cutaneous squamous cell carcinoma. Part 1: Diagnostics and prevention – update 2023. *Eur J Cancer* 2023; **193**:113251.
8 Stratigos AJ, Garbe C, Dessinioti C *et al.* European consensus-based interdisciplinary guideline for invasive cutaneous squamous cell carcinoma: Part 2. Treatment – update 2023. *Eur J Cancer* 2023; **193**:113252.
9 Basset-Seguin N, Maubec E. Recent advanced in the treatment of advanced SCC tumors. *Cancers* 2022; **14**:550.
10 Hillen U, Leiter U, Haase S *et al.* Advanced cutaneous squamous cell carcinoma: a retrospective analysis of patient profiles and treatment patterns – results of a non-interventional study of the DeCOG. *Eur J Cancer* 2018; **96**:34–43.
11 Gentric G, Mieulet V, Mechta-Grigoriou F. Heterogeneity in cancer metabolism: new concepts in an old field. *Antioxid Redox Signal* 2017; **26**:462–85.
12 Obre E, Rossignol R. Emerging concepts in bioenergetics and cancer research: metabolic flexibility, coupling, symbiosis, switch, oxidative tumors, metabolic remodeling, signaling and bioenergetic therapy. *Int J Biochem Cell Biol* 2015; **59**:167–81.
13 Hosseini M, Kasraian Z, Rezvani HR. Energy metabolism in skin cancers: a therapeutic perspective. *Biochim Biophys Acta Bioenerg* 2017; **1858**:712–22.
14 Vander Heiden MG, Cantley LC, Thompson CB. Understanding the Warburg effect: the metabolic requirements of cell proliferation. *Science* 2009; **324**:1029–33.
15 Ward PS, Thompson CB. Metabolic reprogramming: a cancer hallmark even Warburg did not anticipate. *Cancer Cell* 2012; **21**:297–308.
16 Smolkova K, Plecita-Hlavata L, Bellance N *et al.* Waves of gene regulation suppress and then restore oxidative phosphorylation in cancer cells. *Int J Biochem Cell Biol* 2011; **43**:950–68.
17 Hosseini M, Dousset L, Mahfouf W *et al.* Energy metabolism rewiring precedes UVB-induced primary skin tumor formation. *Cell Rep* 2018; **23**:3621–34.
18 Vasan K, Werner M, Chandel NS. Mitochondrial metabolism as a target for cancer therapy. *Cell metabolism* 2020; **32**:341–52.
19 Kaplan MJ. Leflunomide Aventis Pharma. *Curr Opin Investig Drugs* 2001; **2**:222–30.
20 Schiff MH, Strand V, Oed C, Loew-Friedrich I. Leflunomide: efficacy and safety in clinical trials for the treatment of rheumatoid arthritis. *Drugs Today (Barc)* 2000; **36**:383–94.
21 Hosseini M, Dousset L, Michon P *et al.* UVB-induced DHODH upregulation, which is driven by STAT3, is a promising target for chemoprevention and combination therapy of photocarcinogenesis. *Oncogenesis* 2019; **8**:52.
22 Kim J, DeBerardinis RJ. Mechanisms and implications of metabolic heterogeneity in cancer. *Cell Metab* 2019; **30**:434–46.
23 Zoni E, Minoli M, Bovet C *et al.* Preoperative plasma fatty acid metabolites inform risk of prostate cancer progression and may be used for personalized patient stratification. *BMC Cancer* 2019; **19**:1216.
24 Amoedo ND, Sarlak S, Obre E *et al.* Targeting the mitochondrial trifunctional protein restrains tumor growth in oxidative lung carcinomas. *J Clin Invest* 2021; **131**:e133081.
25 Hensley CT, Faubert B, Yuan Q *et al.* Metabolic heterogeneity in human lung tumors. *Cell* 2016; **164**:681–94.
26 Gentric G, Kieffer Y, Mieulet V *et al.* PML-regulated mitochondrial metabolism enhances chemosensitivity in human ovarian cancers. *Cell Metab* 2019; **29**:156–73.
27 Ozisik O, Térézol M, Baudot A. orsum: a Python package for filtering and comparing enrichment analyses using a simple principle. *BMC Bioinformatics* 2022; **23**:293.
28 Medhat W, Hassan A, Korashy H. Sentiment analysis algorithms and applications: a survey. *Ain Shams Eng J* 2014; **5**:1093–113.
29 Karp PD, Billington R, Caspi R *et al.* The BioCyc collection of microbial genomes and metabolic pathways. *Brief Bioinform* 2019; **20**:1085–93.

30 Li YY, Hanna GJ, Laga AC *et al.* Genomic analysis of metastatic cutaneous squamous cell carcinoma. *Clin Cancer Res* 2015; **21**:1447–56.
31 Pickering CR, Zhou JH, Lee JJ *et al.* Mutational landscape of aggressive cutaneous squamous cell carcinoma. *Clin Cancer Res* 2014; **20**:6582–92.
32 Inman GJ, Wang J, Nagano A *et al.* The genomic landscape of cutaneous SCC reveals drivers and a novel azathioprine associated mutational signature. *Nat Commun* 2018; **9**:3667.
33 Shimizu T, Izumi H, Oga A *et al.* Epidermal growth factor receptor overexpression and genetic aberrations in metastatic squamous-cell carcinoma of the skin. *Dermatology* 2001; **202**:203–6.
34 Zhang H, Liu T, Zhang Z *et al.* Integrated proteogenomic characterization of human high-grade serous ovarian cancer. *Cell* 2016; **166**:755–65.
35 Chen SF, Perrella FW, Behrens DL, Papp LM. Inhibition of dihydroorotate dehydrogenase activity by brequinar sodium. *Cancer Res* 1992; **52**:3521–7.
36 Dexter DL, Hesson DP, Ardecky RJ *et al.* Activity of a novel 4-quinolinecarboxylic acid, NSC 368390 [6-fluoro-2-(2′-fluoro-1,1′-biphenyl-4-yl)-3-methyl-4-quinolinecarboxylic acid sodium salt], against experimental tumors. *Cancer Res* 1985; **45**:5563–8.
37 Braakhuis BJM, van Dongen GAMS, Peters GJ *et al.* Antitumor activity of brequinar sodium (Dup-785) against human head and neck squamous cell carcinoma xenografts. *Cancer Lett* 1990; **49**:133–7.
38 Hanson K, Robinson SR, Al-Yousuf K *et al.* The anti-rheumatic drug, leflunomide, synergizes with MEK inhibition to suppress melanoma growth. *Oncotarget* 2017; **9**:3815–29.
39 Strawn LM, Kabbinavar F, Schwartz DP *et al.* Effects of SU101 in combination with cytotoxic agents on the growth of subcutaneous tumor xenografts. *Clin Cancer Res* 2000; **6**:2931–40.
40 Peters GJ, Schwartsmann G, Nadal JC *et al. In vivo* inhibition of the pyrimidine de novo enzyme dihydroorotic acid dehydrogenase by brequinar sodium (DUP-785; NSC 368390) in mice and patients. *Cancer Res* 1990; **50**:4644–9.
41 Shen HSL, Brentzel HJ, Kuhn JG *et al.* Phase I clinical and pharmacokinetic trial of brequinar sodium (DUP 785; NSC 368390). *Cancer Res* 1989; **49**:4648–53.
42 Schwartsmann G, van der Vijgh WJF, van Hennik MB *et al.* Pharmacokinetics of brequinar sodium (NSC 368390) in patients with solid tumors during a phase I study. *Eur J Cancer Clin Oncol* 1989; **25**:1675–81.
43 Sykes DB, Kfoury YS, Mercier FE *et al.* Inhibition of dihydroorotate dehydrogenase overcomes differentiation blockade in acute myeloid leukemia. *Cell* 2016; **167**:171–86.
44 Brown KK, Spinelli JB, Asara JM, Toker A. Adaptive reprogramming of de novo pyrimidine synthesis is a metabolic vulnerability in triple-negative breast cancer. *Cancer Discov* 2017; **7**:391–9.
45 Koundinya M, Sudhalter J, Courjaud A *et al.* Dependence on the pyrimidine biosynthetic enzyme DHODH is a synthetic lethal vulnerability in mutant KRAS-driven cancers. *Cell Chem Biol* 2018; **25**:705–17.
46 Wang X, Yang K, Wu Q *et al.* Targeting pyrimidine synthesis accentuates molecular therapy response in glioblastoma stem cells. *Sci Transl Med* 2019; **11**:eaau4972.
47 White RM, Cech J, Ratanasirintrawoot S *et al.* DHODH modulates transcriptional elongation in the neural crest and melanoma. *Nature* 2011; **471**:518–22.
48 Qiu X, Jiang S, Xiao Y *et al.* SOX2-dependent expression of dihydroorotate dehydrogenase regulates oral squamous cell carcinoma cell proliferation. *Int J Oral Sci* 2021; **13**:3.
49 Mohamad Fairus AK, Choudhary B, Hosahalli S *et al.* Dihydroorotate dehydrogenase (DHODH) inhibitors affect ATP depletion, endogenous ROS and mediate S-phase arrest in breast cancer cells. *Biochimie* 2017; **135**:154–63.
50 Dousset L, Mahfouf W, Younes H *et al.* Energy metabolism rewiring following acute UVB irradiation is largely dependent on nuclear DNA damage. *Free Radic Biol Med* 2024; **227**:459–71.
51 Yamaguchi N, Weinberg EM, Nguyen A *et al.* PCK1 and DHODH drive colorectal cancer liver metastatic colonization and hypoxic growth by promoting nucleotide synthesis. *Elife* 2019; **8**:e52135.